

## Electronic Supporting Information

### Table of contents

**Figure S1.** Experimental (black line) and simulated from single-crystal data (red line) powder X-ray diffraction patterns for  $\{[\text{Mn}^{\text{II}}(\text{H}_2\text{O})_2]_2[\text{Nb}^{\text{IV}}(\text{CN})_8]\cdot 4\text{H}_2\text{O}\}_n$  (room temperature data).

**Figure S2.** Experimental (black line) and simulated from single-crystal data (violet line) powder X-ray diffraction patterns for  $\{[\text{Fe}^{\text{II}}(\text{H}_2\text{O})_2]_2[\text{Nb}^{\text{IV}}(\text{CN})_8]\cdot 4\text{H}_2\text{O}\}_n$  (room temperature data).

**Figure S3.** FT-IR spectra of  $\{[\text{Mn}^{\text{II}}(\text{H}_2\text{O})_2]_2[\text{Nb}^{\text{IV}}(\text{CN})_8]\cdot 4\text{H}_2\text{O}\}_n$  (red) and  $\{[\text{Fe}^{\text{II}}(\text{H}_2\text{O})_2]_2[\text{Nb}^{\text{IV}}(\text{CN})_8]\cdot 4\text{H}_2\text{O}\}_n$  (violet) recorded in KBr pellets with a tentative band assignment

**Figure S4.** Magnetization vs field measured at 2 K for  $\{[\text{Fe}^{\text{II}}(\text{H}_2\text{O})_2]_2[\text{Nb}^{\text{IV}}(\text{CN})_8]\cdot 4\text{H}_2\text{O}\}_n$  and  $\{[\text{Mn}^{\text{II}}(\text{H}_2\text{O})_2]_2[\text{Nb}^{\text{IV}}(\text{CN})_8]\cdot 4\text{H}_2\text{O}\}_n$

**Figure S5.** Polynomial regression of  $M(H^{-1})$  for  $\{[\text{Fe}^{\text{II}}(\text{H}_2\text{O})_2]_2[\text{Nb}^{\text{IV}}(\text{CN})_8]\cdot 4\text{H}_2\text{O}\}_n$  for  $M > 6.5 \mu_B$  (details in the inset) and the resulting  $M_s$  value of  $9.46 \mu_B$  as a limit of the  $M(H^{-1})$  function for  $H^{-1} \rightarrow 0$ .

**Figure S6.** Temperature dependence of magnetic entropy change of  $\text{Mn}^{\text{II}}\text{-L}-[\text{Nb}^{\text{IV}}(\text{CN})_8]$  series, where L= imidazole (imH), pyridazine (pydz) and pyrazole.

**Table S1.** Values of  $T_{r1}$  and  $T_{r2}$  used for the construction of phenomenological universal curve of entropy.

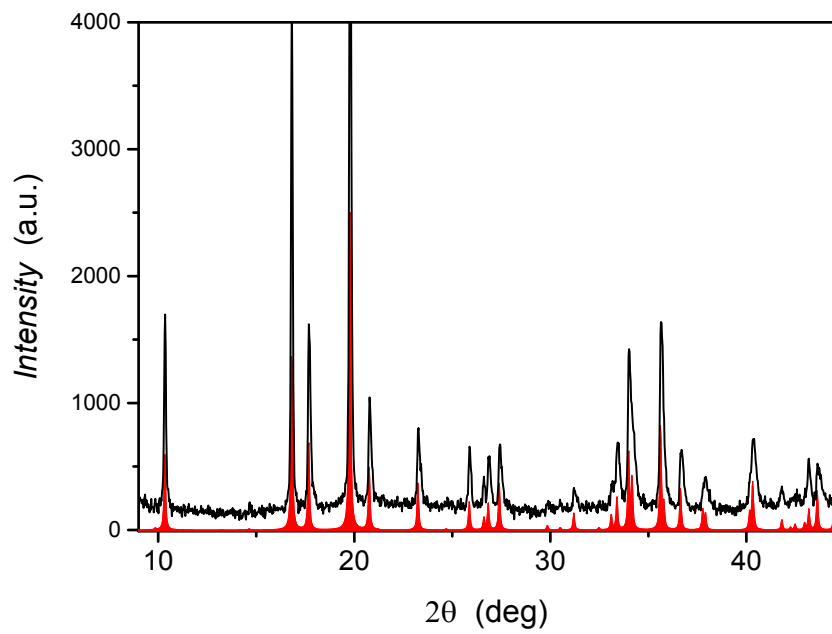


**Figure S1.** Experimental (black line) and simulated from single-crystal data (red line) powder X-ray diffraction patterns for  $\{[\text{Mn}^{\text{II}}(\text{H}_2\text{O})_2]_2[\text{Nb}^{\text{IV}}(\text{CN})_8]\cdot 4\text{H}_2\text{O}\}_n$  (room temperature data).

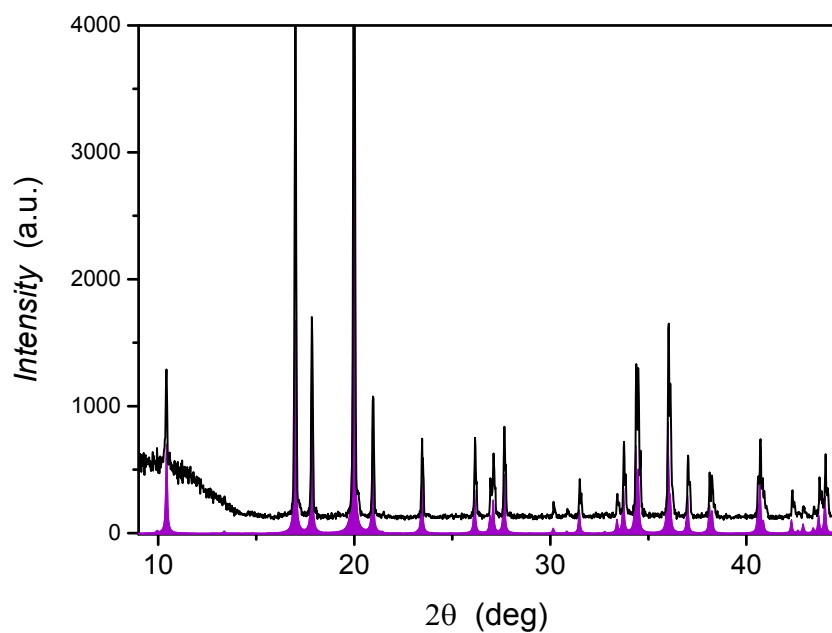


**Figure S2.** Experimental (black line) and simulated from single-crystal data (violet line) powder X-ray diffraction patterns for  $\{[\text{Fe}^{\text{II}}(\text{H}_2\text{O})_2]_2[\text{Nb}^{\text{IV}}(\text{CN})_8]\cdot 4\text{H}_2\text{O}\}_n$  (room temperature data).

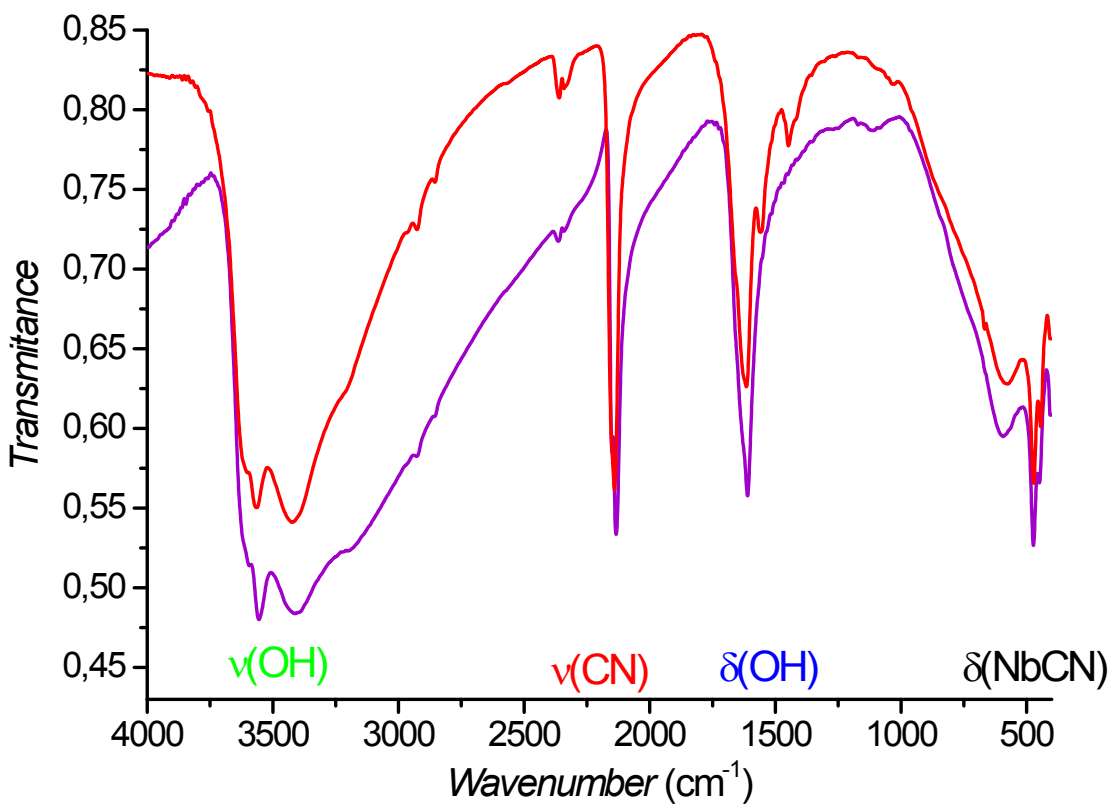


**Figure S3.** FT-IR spectra of  $\{[\text{Mn}^{\text{II}}(\text{H}_2\text{O})_2]_2[\text{Nb}^{\text{IV}}(\text{CN})_8]\cdot 4\text{H}_2\text{O}\}_n$  (red) and  $\{[\text{Fe}^{\text{II}}(\text{H}_2\text{O})_2]_2[\text{Nb}^{\text{IV}}(\text{CN})_8]\cdot 4\text{H}_2\text{O}\}_n$  (violet) recorded in KBr pellets with a tentative band assignment.

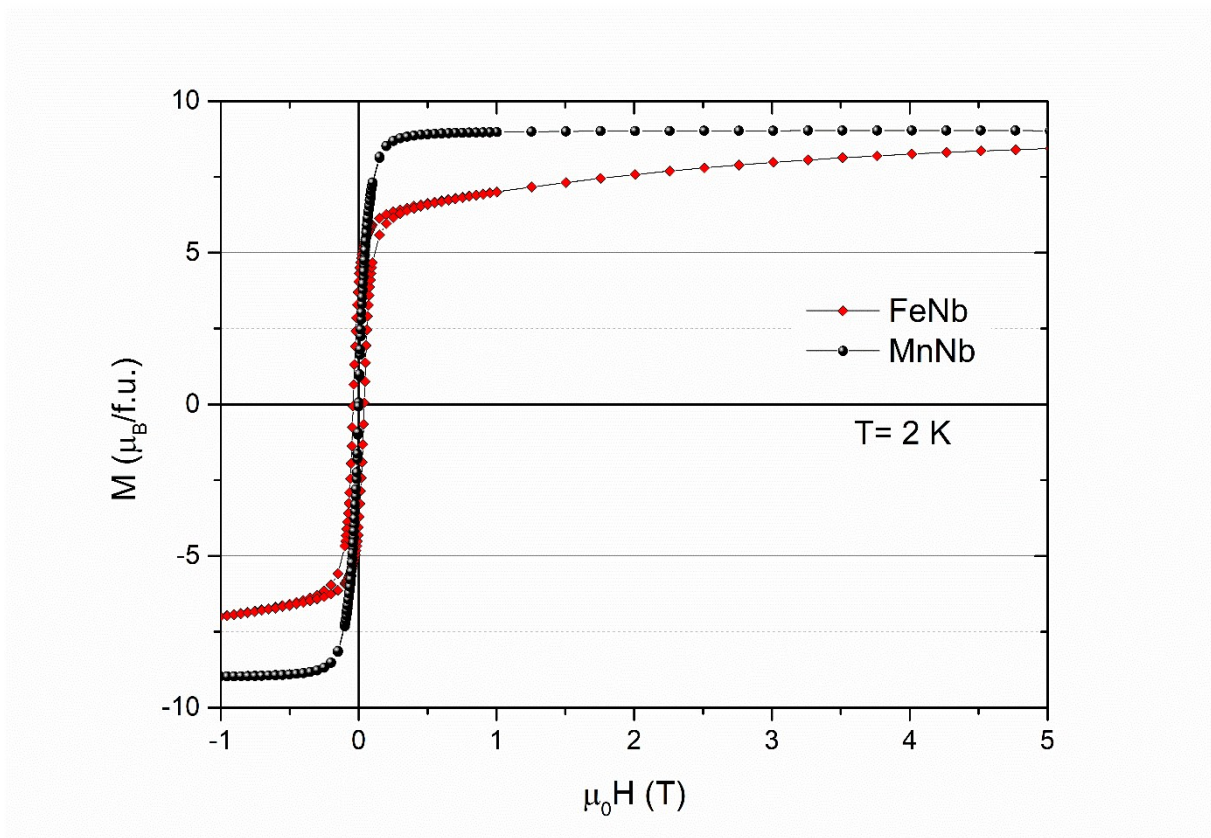


**Figure S4.** Magnetization vs field measured at 2 K for  $\{\text{Fe}^{\text{II}}(\text{H}_2\text{O})_2\}_2[\text{Nb}^{\text{IV}}(\text{CN})_8]\cdot 4\text{H}_2\text{O}\}_n$  and  $\{\text{Mn}^{\text{II}}(\text{H}_2\text{O})_2\}_2[\text{Nb}^{\text{IV}}(\text{CN})_8]\cdot 4\text{H}_2\text{O}\}_n$ .

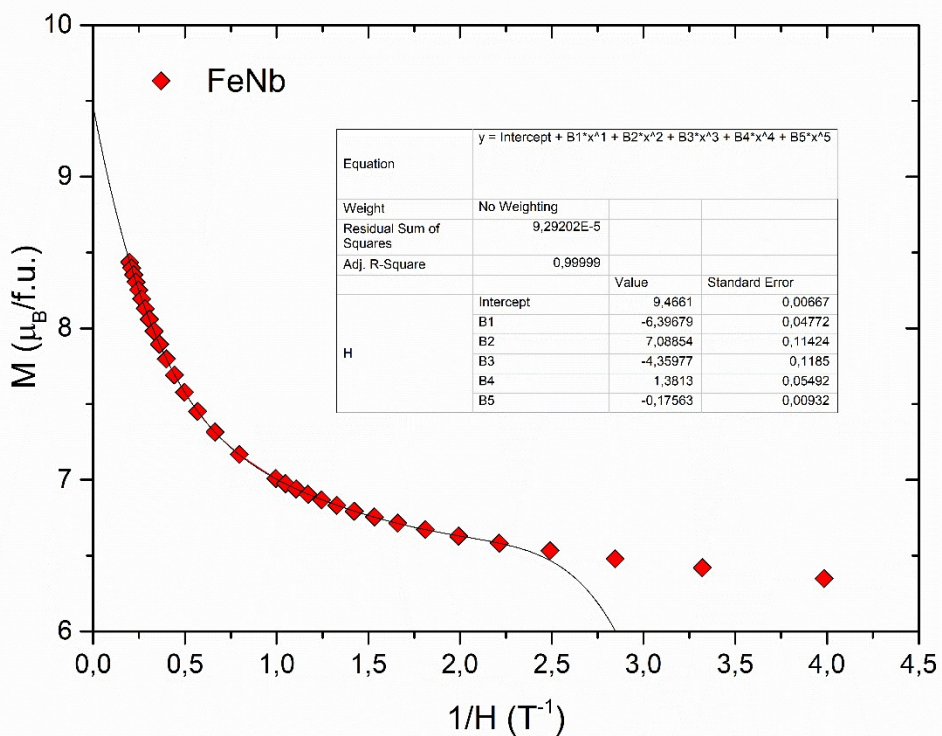


**Figure S5.** Polynomial regression of  $M(H^{-1})$  for  $\{\text{Fe}^{\text{II}}(\text{H}_2\text{O})_2\}_2[\text{Nb}^{\text{IV}}(\text{CN})_8]\cdot 4\text{H}_2\text{O}\}_n$  for  $M > 6.5 \mu_B$  (details in the inset) and the resulting  $M_s$  value of  $9.46 \mu_B$  as a limit of the  $M(H^{-1})$  function for  $H^{-1} \rightarrow 0$ .

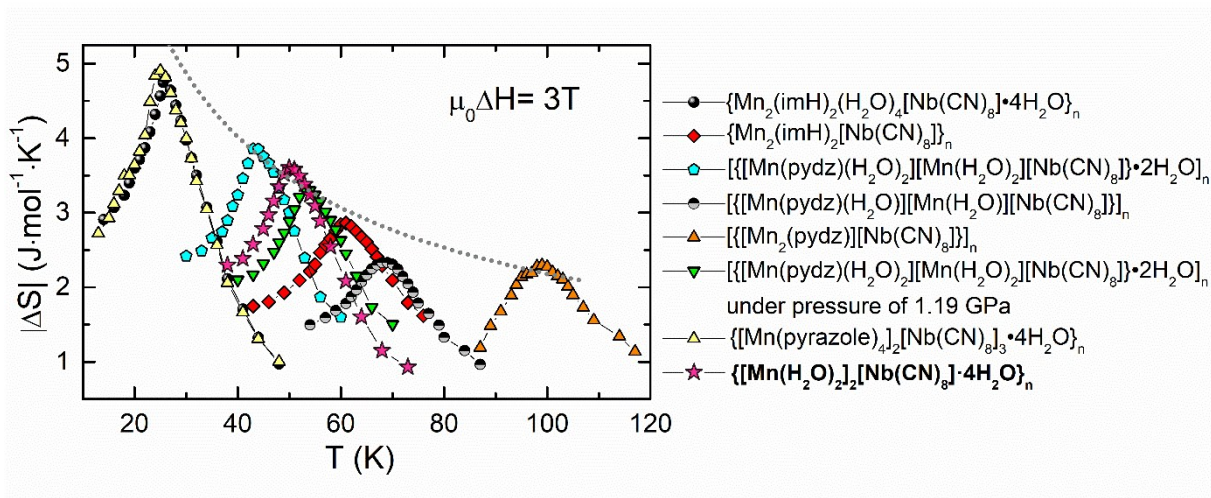


**Figure S6.** Temperature dependence of magnetic entropy change of MnII-L-[NbIV(CN)<sub>8</sub>] series, where L= imidazole (imH), pyridazine (pydz) and pyrazole. Dot line presents the function  $f(T)=A \cdot T^{-2/3}$

**Table S1.** Values of  $T_{r1}$  and  $T_{r2}$  used for the construction of phenomenological universal curve of entropy.

| $\mu_0\text{H}$<br>[T] | MnNb            |                 | FeNb            |                 |
|------------------------|-----------------|-----------------|-----------------|-----------------|
|                        | $T_{r1}$<br>[K] | $T_{r2}$<br>[K] | $T_{r1}$<br>[K] | $T_{r2}$<br>[K] |
| 0.5                    | 46.88           | 51.78           | 40.66           | 47.17           |
| 1                      | 46.59           | 52.95           | 40.23           | 48.28           |
| 2                      | 46.01           | 54.74           | 39.23           | 50.64           |
| 3                      | 45.51           | 56.01           | 38.36           | 52.90           |
| 4                      | 45.10           | 57.28           | 37.56           | 54.58           |
| 5                      | 44.50           | 58.50           | 36.94           | 56.13           |